

## Experimental Study on Nuclear Properties of Water Cooled Pebble Bed Blanket

S. Sato, Y. Verzilov, K. Ochiai, M. Wada, N. Kubota, K. Kondo, M. Yamauchi, T. Nishitani,

Japan Atomic Energy Agency, Tokai-mura, Naka-gun, Ibaraki-ken, 319-1195 Japan

e-mail: sato.satoshi92@jaea.go.jp

**Abstract.** For the first time, nuclear properties are experimentally examined on the water cooled pebble bed blanket by using DT neutrons with two partial mockups; multi-layered mockup with water and pebble bed mockup. Prediction uncertainties are clarified on tritium production rate (TPR) through the experimental analyses. From the multi-layered mockup experiment, it is found that integrated tritium productions can be accurately evaluated. Calculation methods are discussed on the evaluation for TPR of the pebble bed layer, and the precise modeling method is proposed using the hexagonal close-packed heterogeneous geometry. The integrated tritium productions by the homogenous geometry decrease compared with those by the heterogeneous geometry. It is clarified that evaluations are required on a tritium breeding ratio in the blanket design calculation by the proposed method.

### 1. Introduction

In fusion DEMO reactors, the blanket is required to provide a tritium breeding ratio (TBR) more than unity. The water cooled pebble bed blanket being developed by JAEA consists of  $\text{Li}_2\text{TiO}_3$  or  $\text{Li}_2\text{O}$  pebbles with enriched  $^6\text{Li}$  as tritium breeder, beryllium pebbles as neutron multiplier, ferritic steel F82H and water [1]. The TBR is 1.0-1.2 for the present DEMO reactor design, therefore a prediction uncertainty is required to be less than 10 % [1, 2]. The prediction uncertainty is estimated to be more than 10 % based on our previous experiments [3 - 6], and studies have been performed for enhancement of the accuracy [7]. Neutronics experiments were conducted on simple mockup by using DT neutrons in the previous studies [3 - 7]. In those studies, preliminary experimental data were obtained on TPR. In the present study, neutronics experiments have been extended to introduce water and pebble bed layers so that the experimental mockup can better simulate the blanket structure and TPR can be obtained in more detail. Fast neutrons are moderated by water, and slow neutrons increase. TPRs are required to be measured on the blanket including water. In addition, no experimental studies have been reported so far about the pebble bed layer. Since mean free path of slow neutrons is very short in the tritium breeder, TPRs are expected to be affected by the geometry of the breeder. In order to evaluate TPR on the blanket with water and pebble bed layer, neutronics studies are performed on the followings; 1) multi-layered blanket mockup experiment with water panel, 2) pebble bed layer experiment.

### 2. Multi-layered Blanket Mockup Experiment with Water Panel

#### 2.1. Experiment

DT neutron irradiations were performed by using the 80° beam line of the Fusion Neutronics Source (FNS) facility [8] in JAEA. DT neutron yield of the source target was about  $1 \times 10^{11}$  neutrons/s on average. Figure 1 shows the experimental assembly. The mockup is composed of slabs of 16 mm thick first wall panel, two 12 mm thick  $\text{Li}_2\text{TiO}_3$  ( $^6\text{Li}$  enrichment of 40 %) layers, two 101.6 mm thick beryllium layers and four 7.8 mm thick partition panels with 500 mm height and 500 mm width each. The first wall and partition panels are composed

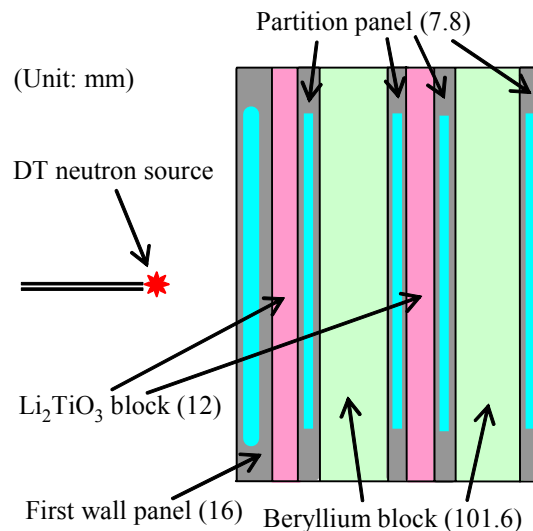


FIG. 1. Cross-sectional view of experimental assembly in the multi-layered blanket mockup.

of F82H and water, and water is filled in the F82H vessel. Thicknesses of the water are 6 and 4.2 mm in the first wall and partition panels, respectively. Front and rear walls are 3 and 7 mm in thickness, respectively, in the first wall panel, and both walls are 1.8 mm in thickness in the partition panels. The partition panels are installed at the boundaries between  $\text{Li}_2\text{TiO}_3$  and beryllium layers. The distance from the DT source to the mockup surface is 100 mm.

As detectors of TPR,  $\text{Li}_2\text{CO}_3$  pellets have been applied. Fifteen slices of  $\text{Li}_2\text{CO}_3$  diagnostic pellets, 13 mm in diameter and 0.5, 1 and 2 mm in thickness, were embedded inside the center of the  $\text{Li}_2\text{TiO}_3$  layers. The lithium isotopes are also enriched by mixing each isotope in these pellets to be equal to the atomic density in the  $\text{Li}_2\text{TiO}_3$ . Tritium activities produced in these irradiated pellets were measured with a liquid scintillation counter (LSC) after the wet-chemistry treatment procedure, thus evaluating TPRs.

## 2.2. Results and Discussions

Numerical analyses were conducted by using Monte Carlo code MCNP-4C [9] with the Evaluated Nuclear Data Libraries FENDL-2.0 [10], JENDL-3.2 [11] and 3.3 [12]. Figure 2 shows distributions of the experimental and calculated values on TPRs. Experimental errors are 7%, which are mainly from the calibration error of the tritium activity measurement. The TPRs increase with decrease in distance to the beryllium layer, and these sharply change in the 12 mm thick breeder layers. The TPRs at the boundaries between the breeder layer and the partition panel adjacent to the beryllium layer are larger than those at the center in the breeder layer by factors of 8 and 6 in the first and second layers, respectively. Table I shows the integrated tritium productions from all the diagnostic pellets. The integrated tritium production in the second layer is 1.3 times as large as that in the first layer. First breeder layer is sandwiched by the first wall panel and the partition panel adjacent to the beryllium layer. On the other hand, second breeder layer is sandwiched by the partition panel adjacent to the beryllium layers. Slow neutrons drastically increase by the reaction between fast neutron and beryllium. The integrated tritium production in the second layer is larger because increased neutrons incident to the breeder layer from both sides.

Figure 3 shows distributions of the ratios of the calculation results to the experimental results (C/Es) on TPRs for the FENDL-2.0. The C/Es are 0.87 – 1.05 in the first layer, and 0.97 – 1.11 in the second layer. Most of the calculation results agree with the experimental results

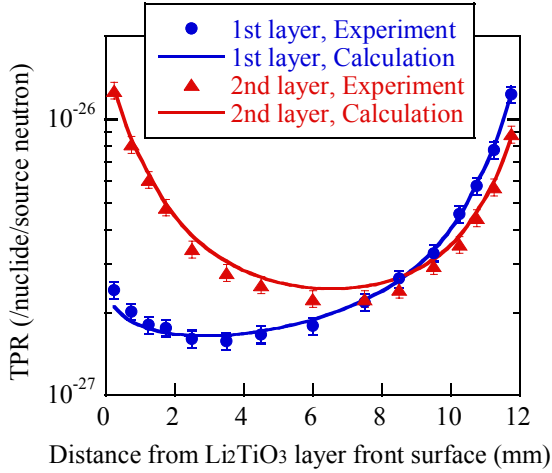


FIG. 2. TPR Distributions.

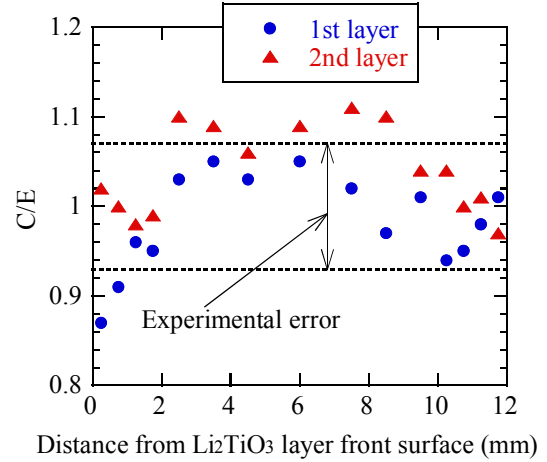


FIG. 3. C/Es on TPRs.

TABLE I: EXPERIMENT AND CALCULATION RESULTS ON INTEGRATED TRITIUM PRODUCTIONS IN MULTI-LAYERED BLANKET MOCKUP EXPERIMENT

	Experiment	Calculation			C/E		
		FENDL-2	JENDL-3.2	JENDL-3.3	FENDL-2	JENDL-3.2	JENDL-3.3
1 <sup>st</sup> layer	6.49	6.44	6.07	6.46	0.99	0.94	0.99
2 <sup>nd</sup> layer	8.70	9.02	8.81	9.07	1.04	1.01	1.04
Total	15.2	15.5	14.9	15.5	1.02	0.98	1.02

Unit:  $\times 10^{20}$  Bq/source neutron

within the experimental error. The C/Es are 0.99 and 1.04 in the first and second layers, respectively, on the integrated tritium productions. The C/E is 1.02 on the tritium production integrated in the first and second breeder layers. Calculations by JENDL-3.2 and 3.3 show the similar results. The prediction uncertainties were clarified on TPRs for the blanket with water from this experimental study. It can be concluded that TPRs are accurately predicted using the latest Monte Carlo code with the nuclear data libraries.

### 3. Pebble Bed Layer Experiment

#### 3.1. Experiment

Nuclear property experiments have been performed using the pebble bed layer mockup. Figure 4 shows the experimental assembly. The mockup is composed of 15 mm thick  $\text{Li}_2\text{O}$  (natural enrichment) pebble bed layer, 101.6 mm thick beryllium block and 1.8 mm thick F82H container. The pebble diameter is 1 mm, and the packing fraction is 57.8 %. The  $\text{Li}_2\text{O}$  pebbles are packed in the F82H container. The beryllium blocks are installed in the both sides of the F82H container. Figure 5 shows the photograph of the pebble bed layer in packing  $\text{Li}_2\text{O}$  pebbles inside the F82H container. The pebble bed layer is 350 mm in height and 350 mm in width. The distance from the DT source to the mockup surface is 100 mm. In order to measure a spatial distribution of TPR in the pebble bed layer, two aluminum cylinders with a thin wall (0.1 mm) filled with pebbles and sectioned on eight equal parts with a diameter of 13 mm and a width of 1.85 mm were installed at the center of the pebble bed layer (Detector #1) and at the position of 29 mm distance from the center in the horizontal direction (Detector #2). Tritium activities produced in the pebbles were measured with a LSC.

### 3.2. Numerical Calculation

The experiment was analyzed by MCNP-4C with homogeneous and heterogeneous geometries for the pebble bed layer. Homogenous geometries have been applied in the blanket design calculation. By mixing the void and the pebble, i. e. diluting the atomic density in the pebble bed layer, homogeneous geometries have been created. A hexagonal close-packed model was assumed in the heterogeneous geometry, and all pebbles and void among the pebbles were simulated using the repeated-structure modeling method. Figure 6 shows zoomed-up cross-sectional views of the hexagonal close-packed heterogeneous geometry applied for MCNP calculation in this study. Pebble bed layers are created by repeating the unit cell shown in bold lines. Yellow means the pebble bed layer, and green means the pebble for the TPR detector. The pebble packing fraction is 74 % in the hexagonal close-packed models, while it is 57.8 % in the experiment. It is proposed that uniform annular gaps are installed at the boundaries between adjacent pebbles in the calculation to adjust the packing fraction in the experiment.

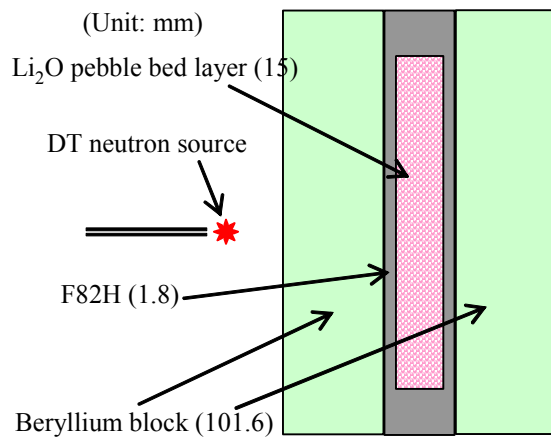


FIG. 4. Cross-sectional view of experimental assembly in the pebble bed layer experiment.

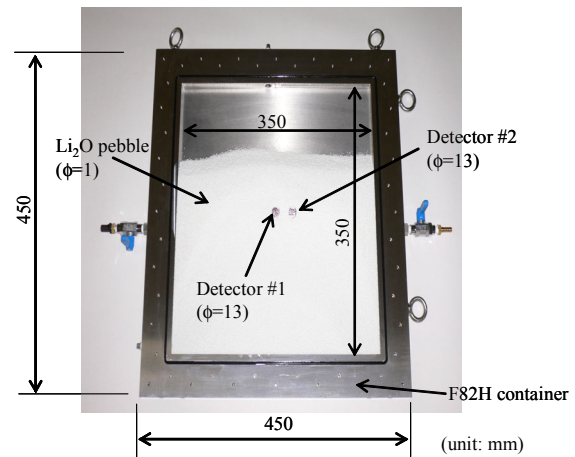


FIG. 5. Photograph of the pebble bed layer in packing Li<sub>2</sub>O pebbles inside the F82H container.

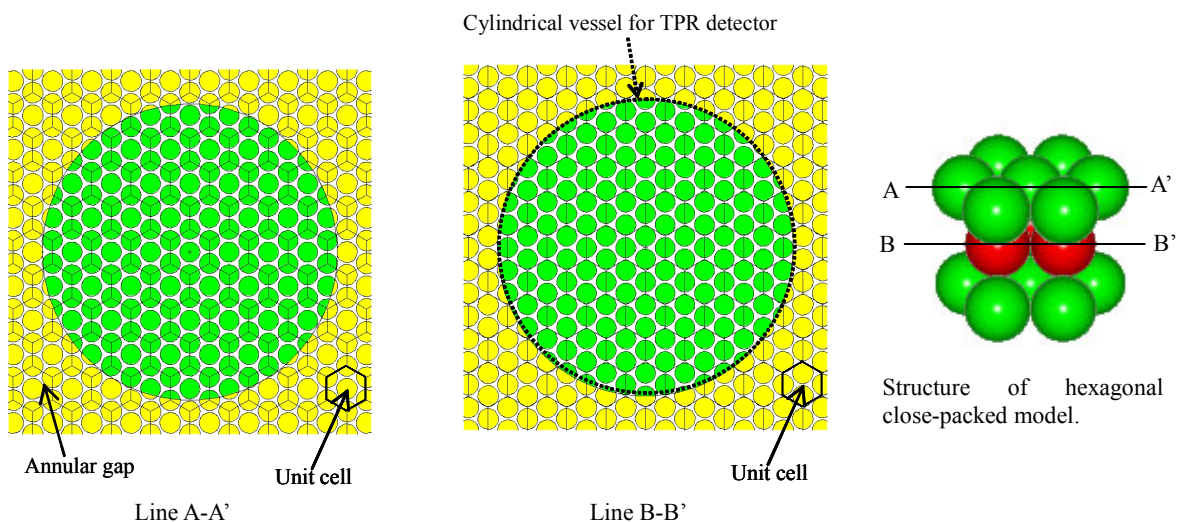


FIG. 6. Cross-sectional views of the hexagonal close-packed heterogeneous calculation geometry applied for MCNP in the pebble bed layer blanket mockup experiment.

### 3.3. Results and Discussions

Figures 7 and 8 show distributions of the experimental and calculation results on the TPRs for the detectors #1 and #2, respectively. Similarly to the results on the multi-layered blanket mockup experiment shown in Fig. 2, the TPRs increase as distance to one of the beryllium layers on both sides decreases. The TPRs at the boundary between the breeder layer and the container are larger than those at the center in the breeder layer by a factor of 1.6. Changes of the TPRs along the depth of the breeder layer in the pebble bed mockup are much lower than those in the multi-layered mockup. This is because atomic density of  ${}^6\text{Li}$  is smaller due to natural isotope and pebble bed layer.

Figures 9 and 10 show distributions of the C/E on the TPRs for the detectors #1 and #2, respectively. The C/E values are 0.91 – 1.05 except for the boundary in the homogeneous and heterogeneous geometries, and most of calculation results agree well with the experimental ones. Table II shows integrated tritium productions from all the diagnostic pellets and these C/Es. The C/Es are 0.97 and 0.99 in the homogeneous and heterogeneous geometries, respectively, on the integrated tritium production.

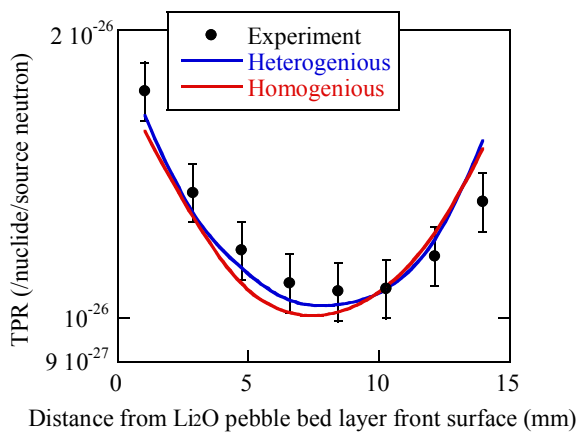


FIG. 7. TPR Distributions in the detector #1.

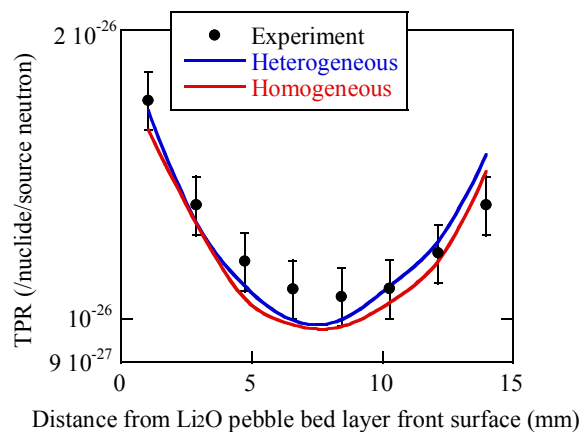


FIG. 8. TPR Distributions in the detector #2.

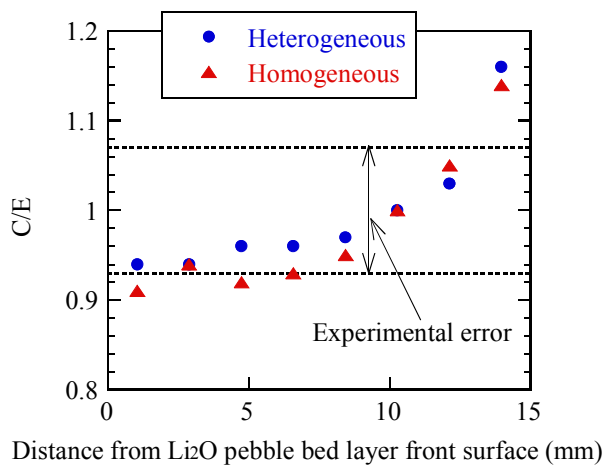


FIG. 9. C/E distributions on TPR in the detector #1.

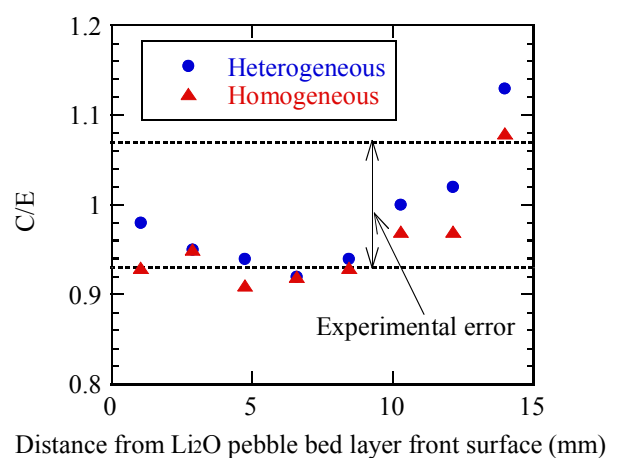


FIG. 10. C/E distributions on TPRs in the detector #2.

TABLE II: EXPERIMENTAL AND CALCULATION RESULTS ON INTEGRATED TRITIUM PRODUCTIONS IN PEBBLE BED MOCKUP EXPERIMENT

	Experiment	Homogeneous geometry		Heterogeneous geometry	
		Calculation	C/E	Calculation	C/E
Detector #1	5.18	5.06	0.98	5.14	0.99
Detector #2	5.11	4.90	0.96	5.04	0.99
Total	10.3	9.96	0.97	10.2	0.99

Unit:  $\times 10^{20}$  Bq/source neutron

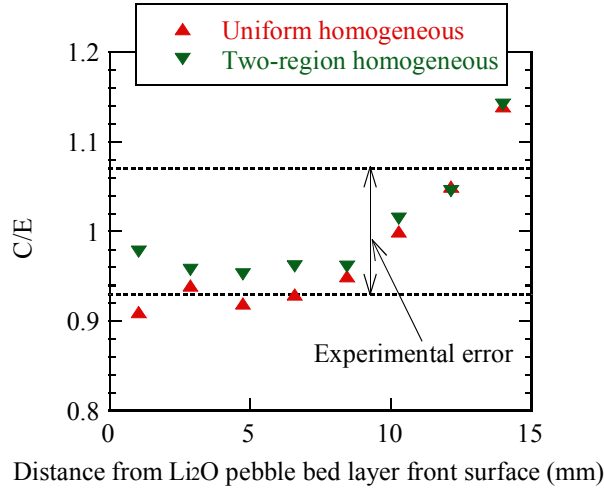


FIG. 11. C/E distributions on TPRs in the detector #1.

At the boundaries between the pebble bed layer and the F82H container, it is observed that the divergence of C/Es from unity is slightly larger. This is expected to be due to change of the packing fraction in the boundary. In order to evaluate this effect, calculations have been performed using a two-region homogeneous geometry. These have been performed changing the packing fraction partially and keeping constant values on the total packing fraction. The packing fraction in the region of 0 – 1.875 mm depth from the front boundary was changed to 50.8 %. The packing fraction in the region of 1.875 – 15 mm depth was changed to 58.8 %. Total packing fraction is 57.8 %. Figure 11 shows distributions of the C/Es in the two-region homogeneous geometry with ones in the uniform homogenous geometry. Calculation results are improved by applying the two-region homogeneous geometry.

Influence of  ${}^6\text{Li}$  enrichment was further studied on integrated tritium production in the calculation. Figure 12 shows ratios of the integrated tritium production with the homogeneous geometry to that with the heterogeneous geometry as a function of the enrichment of  ${}^6\text{Li}$  isotope. This figure shows the results on the tritium productions integrated in the pebble bed layer with dimensions of 15 mm in thickness, 350 mm in width and 350 mm in height. With the increase of the  ${}^6\text{Li}$  enrichment, the difference between integrated tritium productions for the heterogeneous and homogeneous geometries becomes larger. In the case of the 90 % enriched  ${}^6\text{Li}$ , the difference is about 5 %. The effect is due to reduction of the effective macro-scopic tritium production cross section in the homogeneous geometry. Figure 13 shows the ratios as a function of the distance from the  $\text{Li}_2\text{O}$  pebble bed layer front surface. This figure shows the tritium productions integrated in the pebble bed layer with dimensions of

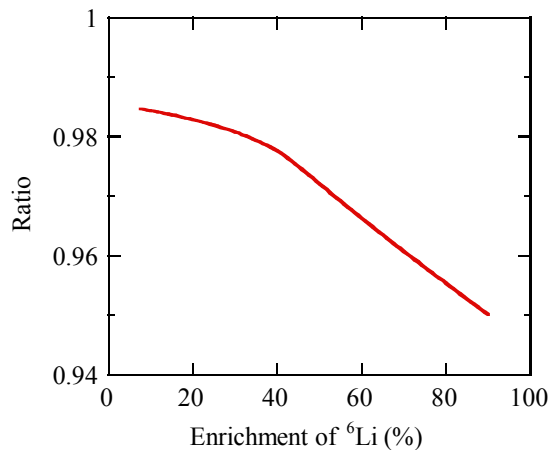


FIG. 12. Ratios of the integrated tritium production with the homogeneous geometry to that with the heterogeneous geometry in the pebble bed layer.

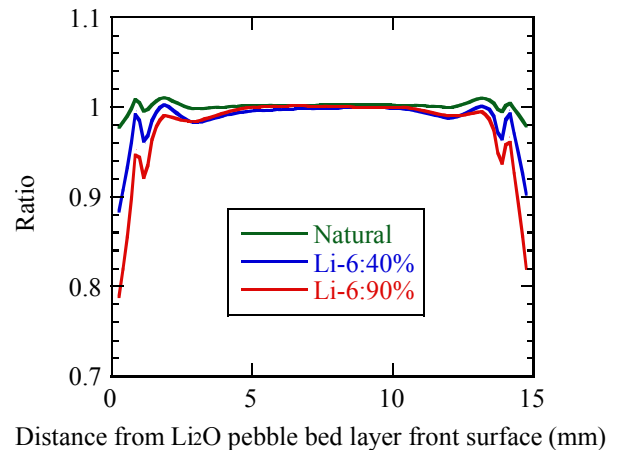


FIG. 13. Ratio of the integrated tritium production with the homogeneous geometry to that with the heterogeneous geometry in the pebble bed layer.

350 mm in width and 350 mm in height in cases of natural, 40 % and 90 % enrichment for  ${}^6\text{Li}$  isotope. In cases of natural, 40 % and 90 % enrichment, the integrated tritium productions with the homogeneous geometry are lower than those with the heterogeneous geometry by more than 2 %, 10 % and 20 % in the boundaries, though no significant differences are found around the center. Mean free path for slow neutrons is less than 1 mm for the  ${}^6\text{Li}(n,\alpha){}^3\text{H}$  reaction, and this is very short. This becomes shorter with the enrichment of  ${}^6\text{Li}$ . Effective atomic densities in the homogeneous geometry decrease compared with those in the heterogeneous geometry in the boundaries. This is because the atomic densities are diluted and the surface area are reduced in the homogenous geometry. It is expected that the decrease of the effective atomic densities reduces tritium productions in the homogeneous geometry.

The heterogeneous calculation method proposed in the present study can enhance calculation accuracy compared with the homogenous geometry, e.g. by 5 % in the case of the 90 % enriched  ${}^6\text{Li}$  for the integrated tritium production, and it can be concluded that this method is essential for evaluations of TPR and TBR in the pebble bed layer.

#### 4. Summary

We have studied nuclear properties of water cooled pebble bed blanket using a DT neutron source. Experiments have been done using two partial mockups; multi-layered mockup with water and pebble bed mockup. Numerical studies have been also performed using the latest Monte Carlo calculation code and nuclear data libraries. As evaluation for the pebble bed layer, a numerical calculation method was proposed using a hexagonal close-packed heterogeneous geometry. From these experiments and numerical studies, following findings have been obtained.

- (1) The C/Es were range of 0.94 - 1.04 on integrated tritium productions from the multi-layered blanket mockup experiment. It was found that integrated tritium productions could be accurately evaluated.
- (2) The C/Es were 0.97 and 0.99 on integrated tritium productions with the homogeneous and heterogeneous geometries, respectively, from the pebble bed mockup experiment. The integrated tritium productions obtained by the homogeneous geometry are smaller than that by the heterogeneous geometry.

- (3) The integrated tritium productions by the homogeneous geometry were clearly reduced compared with those by the heterogeneous geometry in both boundaries between the pebble bed layer and its container. With enrichment, the results the by homogeneous geometry decrease.
- (4) Impact of this reduction due to the homogeneous geometry on the blanket design is not so small, and it can be concluded that Monte Carlo calculations with the heterogeneous geometry is essential on TBR evaluations.

### Acknowledgments

The authors would like to thank Messrs. C. Kutsukake, S. Tanaka, Y. Abe, M. Seki, Y. Oginuma and M. Kawabe for operation of the FNS accelerator. The authors thank Drs. M. Seki, S. Seki and H. Takatsu for their support and encouragement.

### References

- [1] ENOEDA, M., et al., "Design and Technology Development of Solid Breeder Blanket Cooled by Supercritical Water in Japan", Nucl. Fusion **43** (2003)1837.
- [2] YANAGI, Y., et al., "Nuclear and Thermal Analyses of Supercritical-water-cooled Solid Breeder Blanket for Fusion DEMO Reactor", J. Nucl. Sci. Technol. **38** (2001) 1014.
- [3] OCHIAI, K., et al., "Neutronics Experiment of <sup>6</sup>Li-enriched Breeding Blanket with Li<sub>2</sub>TiO<sub>3</sub>/Be/F82H Assembly Using D-T Neutrons", J. Nucl. Sci. Technol. **Suppl.2** (2002) 1147.
- [4] KLIX, A., et al., "Tritium Measurement for <sup>6</sup>Li-Enriched Li<sub>2</sub>TiO<sub>3</sub> Breeding Blanket Experiments with D-T Neutrons", Fusion Sci. Technol., **41** (2002) 1040.
- [5] SATO, S., et al., "Neutronics Experiments for DEMO Blanket at JAERI/FNS", Nucl. Fusion **43** (2003) 527.
- [6] SATO, S., et al., "Experimental Studies on Tungsten-armor Impact on Nuclear Responses of Solid Breeding Blanket", Nucl. Fusion **45** (2005) 656.
- [7] SATO, S., et al., "Neutronics Experiments Using Small Partial Mockups of the ITER Test Blanket Module with a Solid Breeder", Fusion Sci. Technol., **47** (2005) 1046.
- [8] <http://fnshp.tokai-sc.jaea.go.jp/>
- [9] BRIESMEISTER, J. F., "MCNP - A General Monte Carlo N-Particle Transport Code, Version 4C", LA-13709-M, LANL, Los Alamos (2000).
- [10] WIENKE, H., HERMAN, M., "FENDL/MG-2.0 and FENDL/MC-2.0, The Processed Cross Section Libraries for Neutron-photon Transport Calculations, Version 1 of February 1998", IAEA-NDS-176 Rev 0, IAEA, Vienna (1998).
- [11] NAKAGAWA, T., et al., "Japanese Evaluated Nuclear Data Library Version 3 reversion-2: JENDL-3.2", J. Nucl. Sci. Technol. **32** (1995) 1259.
- [12] SHIBATA, K., et al., "Japanese Evaluated Nuclear Data Library Version 3 Revision-3: JENDL-3.3", J. Nucl. Sci. Technol. **39** (2002) 1125.